International Journal of Chronic Obstructive Pulmonary Disease

Dovepress
Taylor & Francis Group

Open Access Full Text Article

ORIGINAL RESEARCH

Nomogram Model for Identifying the Risk of Coronary Heart Disease in Patients with Chronic Obstructive Pulmonary Disease Based on Deep Learning Radiomics and Clinical Data: A Multicenter Study

Hupo Bian[1,2,*], Huiying Qian[2,3,*], Shaoqi Zhu[2,4], Jingnan Xue[1,2], Luying Qi[1,2], Xiuhua Peng[1], Mei Li[1], Yifeng Zheng[3], Pengliang Xu[5], Hongxing Zhao[1,6], Jianping Jiang[7]

[1]Department of Radiology, The First Affiliated Hospital of Huzhou University, Huzhou, Zhejiang, People's Republic of China; [2]School of Medicine (School of Nursing), Huzhou University, Huzhou, Zhejiang, People's Republic of China; [3]Department of Radiology, Huzhou Central Hospital Affiliated to Huzhou University, Huzhou, Zhejiang, People's Republic of China; [4]Department of Endocrinology, The First Affiliated Hospital of Huzhou University, Huzhou, Zhejiang, People's Republic of China; [5]Department of Thoracic Surgery, The First Affiliated Hospital of Huzhou University, Huzhou, Zhejiang, People's Republic of China; [6]Huzhou Key Laboratory of Precise Diagnosis and Treatment of Urinary Tumors, Huzhou, Zhejiang, People's Republic of China; [7]Department of Cardiovascular Center, The First Affiliated Hospital of Huzhou University, Huzhou, Zhejiang, People's Republic of China

*These authors contributed equally to this work

Correspondence: Jianping Jiang, Department of Cardiovascular Center, The First Affiliated Hospital of Huzhou University, No. 158, Plaza Back Road, Wuxing District, Huzhou City, Zhejiang Province, People's Republic of China, Email 2441919792@qq.com

Objective: This study aimed to develop and validate a deep learning radiomics (DLR) nomogram for individualized CHD risk assessment in the COPD population.

Methods: This retrospective study included 543 COPD patients from two different centers. Comprehensive clinical and imaging data were collected for all participants. In Center 1, 398 patients were randomly allocated into a training set and an internal validation set at a 7:3 ratio. An external test set was established using 145 patients from Center 2. Radiomics features were extracted from computed tomography (CT) images, and deep learning features were generated using ResNet50. By integrating traditional clinical data, radiomics features, and three-dimensional (3D) deep learning features, a combined predictive model was developed to estimate the risk of CHD in COPD patients.

Results: Validation cohort AUCs revealed the nomogram's optimal predictive performance (Internal: 0.800; External: 0.761) compared to clinical (0.759, 0.661), radiomics (0.752, 0.666), and DLR (0.767, 0.732) models. This integrative approach demonstrated a 9.1% and 13.4% relative AUC improvement over clinical and radiomics models in external validation. DCA corroborated these findings, showing the nomogram provides the highest net benefit for clinical decision-making across probability thresholds in COPD patients at risk for CHD.

Conclusion: The nomogram model, which integrates clinical, radiomics, and deep learning features, exhibits promising performance in predicting CHD risk among COPD patients. It may offer valuable insights for early intervention and management strategies for CHD.

Keywords: chronic obstructive pulmonary disease, coronary heart disease, deep learning, radiomics, nomogram

Introduction

Chronic obstructive pulmonary disease (COPD) ranks as the third leading cause of death globally and is among the top five diseases imposing the heaviest social burden.[1] Epidemiological studies have demonstrated that the prevalence of

Received: 29 May 2025
Accepted: 24 August 2025
Published: 2 September 2025

COPD in individuals aged 40 years or older in China is approximately 13.7%.[2] COPD frequently coexists with other chronic conditions, including cardiovascular diseases, osteoporosis, diabetes, lung cancer, cachexia, anemia, anxiety, and depression.[3–5] Among these comorbidities, coronary heart disease (CHD) has emerged as a significant comorbidity of COPD, contributing to increased mortality rates and imposing a substantial social burden.[6] Although the precise mechanisms linking COPD and CHD remain unclear, shared risk factors such as smoking, advanced age, and systemic inflammation have been identified.[7] Extensive research has established a positive causal relationship between COPD and CHD, indicating that the presence and progression of CHD may precipitate acute exacerbations of COPD.[8] Consequently, early identification of CHD in COPD patients and timely intervention are of paramount importance.

The rapid advancement of artificial intelligence has generated considerable interest in leveraging radiomics derived from chest CT scans for the study of COPD.[9] Radiomics represents an innovative high-throughput approach for extracting quantitative imaging features,[10,11] which has been successfully applied in various aspects of COPD management, including early diagnosis,[12] staging,[13] and differential diagnosis.[14] Routine chest CT imaging examinations for COPD patients provide a unique opportunity for simultaneous detection of early-stage CHD. Previous studies have developed whole-lung radiomics nomograms to identify cardiovascular diseases in COPD patients.[15] However, deep learning techniques possess the capability to quantify high-dimensional radiological phenotypes beyond human perception, enabling the construction of specialized predictive models tailored to diverse clinical scenarios.[16] To date, no studies have utilized deep learning-based radiomics (DLR) techniques to predict the risk of CHD in COPD patients. This study aims to compare the diagnostic performance of single radiomics and DLR nomograms in identifying CHD in COPD patients.

Materials and Methods

Patients and Clinical Data

This study was approved by the Institutional Review Board of The First People's Hospital of Huzhou (Approval Number: 2025KYLL002-01), and the requirement for informed consent was waived due to the retrospective nature of the research. The study was conducted in accordance with the ethical principles of the Declaration of Helsinki. The clinical data and CT images of eligible patients from the two centers from January 2020 to February 2025 were collected. A total of 543 patients diagnosed with chronic obstructive pulmonary disease (COPD) via pulmonary function tests (PFTs) in the two centers during this period were included in the study. The inclusion criteria were as follows: (1) COPD diagnosis confirmed by PFT; (2) completion of both PFT and chest computed tomography (CT) within a two-week interval; (3) availability of complete thin-slice (1 mm) chest CT images. The exclusion criteria were as follows: (1) incomplete clinical data or presence of other thoracic diseases (eg:pneumonia, atelectasis, pulmonary nodules or masses larger than 6 mm, pleural effusion); (2) history of any malignant tumor; (3) spinal implantation or significant image artifacts affecting diagnostic quality; (4) lack of thin-slice chest CT images; (5) evidence of soft plaque on coronary angiography or coronary computed tomography angiography (CTA). To enhance the rigor of the study and prevent model overfitting, 398 patients from Center 1 were randomly divided into a training cohort (n = 278) and an internal validation cohort (n = 120) in a 7:3 ratio.

Meanwhile, 145 patients from Center 2 were assigned to an external validation cohort (n = 145). The training cohort was used for model development, while the internal and external validation cohorts were employed to evaluate the model's performance in clinical practice and ensure research robustness. Clinical information included age, body mass index (BMI), gender, Global Initiative for Chronic Obstructive Lung Disease (GOLD) grade, and smoking status. Laboratory examination indicators comprised C-reactive protein (CRP), erythrocyte sedimentation rate (ESR), procalcitonin (PCT), albumin, alkaline phosphatase, absolute eosinophil count, triglycerides, platelet distribution width (PDW), arterial partial pressure of carbon dioxide (PaCO2), white blood cell count, neutrophil percentage, lymphocyte percentage, hematocrit, red blood cell distribution width, mean platelet volume, arterial partial pressure of oxygen (PaO2), hemoglobin, and globulin. For missing values, we imputed them using mean substitution. Coronary heart disease (CHD) events were identified by reviewing the first page of inpatient records with a CHD diagnosis. The presence or absence of CHD events was determined upon admission, with the time interval between admission and chest CT scan being less than

one month. CHD events were defined according to the International Classification of Diseases (ICD) (https://icd.who.int/browse/2024-01/mms/en).

CT Image Acquisition and Pulmonary Function Examination

CT Image Acquisition

All participants received non-contrast computed tomography (CT) scans of the entire thorax during maximal inspiration. Scans were performed using one of the following scanners: Aquilion ONE TSX-301C (Canon Medical Systems), Somatom Force (Siemens Healthineers), or Brilliance CT 16 (Philips Healthcare). Detailed scanning parameters are provided in Supplementary Material 1.

Pulmonary Function Assessment

Spirometry was conducted using a Ganshorn PowerCube spirometer. Chronic obstructive pulmonary disease (COPD) diagnosis was established based on a post-bronchodilator forced expiratory volume in 1 second (FEV_1) to forced vital capacity (FVC) ratio (FEV_1/FVC) below 0.7, accompanied by an increase in FEV_1 of less than 200 mL following administration of a bronchodilator.[17]

Participant Stratification

Subjects were categorized according to the Global Initiative for Chronic Obstructive Lung Disease (GOLD) spirometric criteria:[18] GOLD 1 (Mild): $FEV_1/FVC < 0.7$ and $FEV_1 \geq 80\%$ predicted; GOLD 2 (Moderate): $FEV_1/FVC < 0.7$ and $50\% \text{ predicted} \leq FEV_1 < 80\%$ predicted; GOLD 3 (Severe): $FEV_1/FVC < 0.7$ and $30\% \text{ predicted} \leq FEV_1 < 50\%$ predicted; GOLD 4 (Very Severe): $FEV_1/FVC < 0.7$ and $FEV_1 < 30\%$ predicted.

Automatic Segmentation of the Entire Lung

Automated bilateral lung segmentation was implemented via the OnekeyAI platform (https://github.com/OnekeyAI-Platform/onekey), with left and right lungs segmented separately prior to fusion into a composite ROI (Algorithm workflow: Supplementary Material 2). Segmentation fidelity was then independently verified by two thoracic radiologists (each >10 years' experience) using ITK-SNAP (v3.8.0), with manual correction of discordances.[19]

Radiomics and Deep Learning Feature Extraction

Radiomic feature extraction was performed using PyRadiomics (version 3.7.12; https://pyradiomics.readthedocs.io) integrated within the OnekeyAI platform. Three feature classes were extracted: first-order statistics, morphological descriptors, and textural patterns. All features were subjected to Z-score normalization, thereby addressing the heterogeneity of imaging data introduced by multiple centers and multiple scanners, enabling the feature values to have relative comparability and enhancing the performance and stability of the model. Computations were performed on both original images and filtered variants, including wavelet decompositions and Laplacian of Gaussian (LoG) transformations.Prior to feature extraction, images were preprocessed through:Isotropic resampling (1×1×1 mm voxels), Gray-level discretization (fixed bin width: 25 Gy) and Intensity normalization.This preprocessing pipeline standardizes acquisition variability and enhances signal-to-noise ratio across heterogeneous datasets.

The RseNet50 architecture is used to develop convolutional neural networks (CNNS) for extracting features of deep learning, effectively solving the degradation problem in deep networks by using residual blocks. To guarantee the model's effectiveness across diverse patient populations with notable variability, we utilized transfer learning. This involved initializing the model with pre-trained weights from the ImageNet database, thereby enhancing its adaptability to various datasets. A crucial aspect of our method was the precise tuning of the learning rate to improve generalization across datasets. For this, we adopted the cosine decay learning rate strategy. Subsequently, the pre-trained CNN model was used to extract deep learning features for each image with the maximum ROI. We utilized its second-to-last layer for deep learning feature extraction. Figure 1 presents the flowchart of the entire research design.

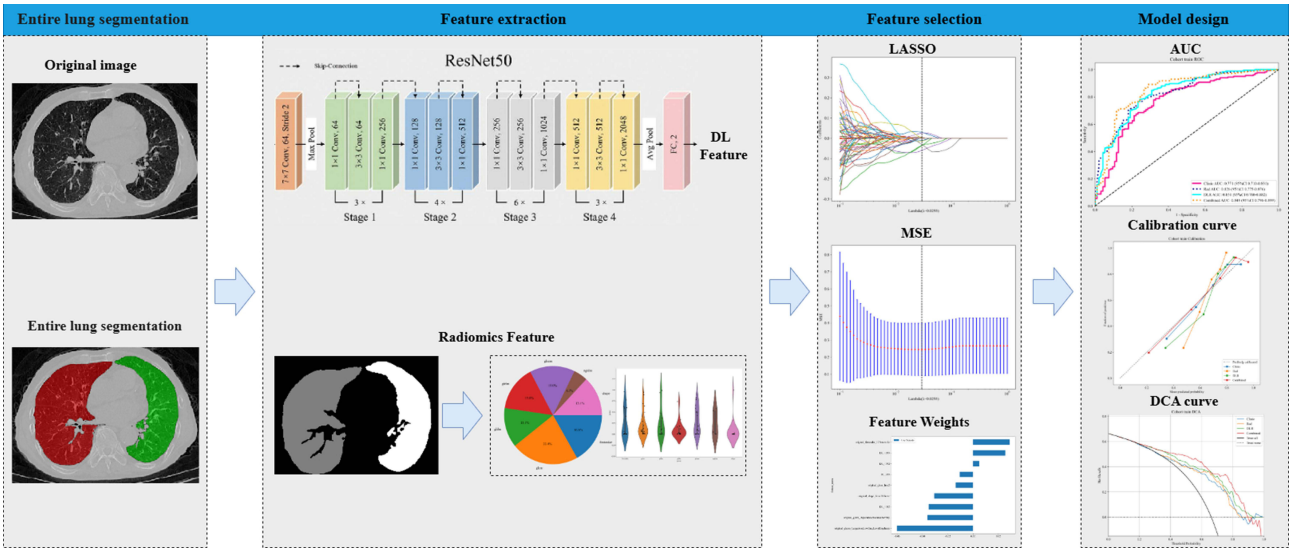

Figure 1 The flowchart of the entire research design.

Radiomics and Deep Learning Feature Selection

All features underwent Z-score normalization. Statistically significant features were identified through univariate analysis (*t*-test; $p<0.05$). To mitigate multicollinearity, features with Pearson correlation coefficients >0.9 were iteratively excluded, retaining only one from each correlated pair. Final feature optimization was achieved via Lasso regression with 10-fold cross-validation, where the regularization parameter λ was tuned to maximize predictive performance while minimizing feature dimensionality. All features with non-zero coefficients retained were used for regression model fitting and combined into radiomics signatures. Subsequently, we retained the features through linear combination and weighted them according to their model coefficients to calculate the radiomics score (rad score, RS) of the patients.

Construction of Clinical Models, Radiomics, Deep Learning Radiomics Models and Nomogram Models

After feature screening, radiomics, DLR, clinical models and combined models were constructed, respectively. Through Logistic regression analysis of clinical characteristics, subsequently, logistic regression analysis was used to determine statistically significant characteristics for the development of clinical models. The machine learning model LightGBM was trained using the selected radiomics features to construct the radiomics model. For constructing the DLR signature, we employed a pre-fusion algorithm that combines deep learning features with radiomic features. Subsequently, we followed a procedure similar to the one used in radiomics for feature selection and model construction. To enhance its clinical relevance, we performed univariable and stepwise multivariable analyses on all clinical features to identify those of significance. By integrating these selected clinical features with the predictions from our DLR model, we developed a Logistic Regression (LR) linear model, culminating in the creation of the Combined Signature. This signature was effectively visualized using a nomogram. The predictive model underwent rigorous clinical validation in the test cohort through:Classification performance: AUC, accuracy (ACC), sensitivity (SEN), specificity (SPE), precision (PPV), recall, and F1-score;Discriminative capacity: ROC curve analysis; Reliability assessment: Calibration curves verified by Hosmer-Lemeshow test; Translational relevance: Decision curve analysis (DCA) evaluating clinical decision-making utility.This multi-faceted validation framework establishes both statistical robustness and practical value.

Statistical Analysis

Normality of clinical features was assessed via Shapiro–Wilk testing. Continuous variables were analyzed using either independent t-tests (normally distributed) or Mann–Whitney *U*-tests (non-normal distributions). Categorical variables underwent χ^2 analysis. Inter-cohort comparability was confirmed (all $p>0.05$), validating unbiased group stratification.

All analyses were executed on the OnekeyAI platform (v4.9.1) with the following computational environment: Python: 3.7.12; Statistical packages: Statsmodels v0.13.2; Radiomics extraction: PyRadiomics v3.7.12; Machine learning: Scikit-learn v1.0.2 (Support Vector Machine implementation); Deep learning: PyTorch v1.11.0 with GPU acceleration (CUDA v11.3.1, cuDNN v8.2.1).

Result

Baseline Characteristics of Patients and Construction of Clinical Models

The flowchart of the patient's selection is shown in Figure 2. As of February 2025, we included a total of 719 patients diagnosed with COPD. After screening based on inclusion and exclusion criteria, the final cohort (n=543) included 87 females and 456 males. The average age of the entire cohort was 75.09 years. Among them, 166 COPD patients had no CHD, while 377 COPD patients had CHD. Table 1 details the baseline clinical characteristics of the study cohort (Standardized units for all indicators in Table 1 are provided in Supplementary Material 5).

Univariate and multivariate analyses were conducted on the clinical characteristics of the training set, and the odds ratio (OR) of each feature and its corresponding P value were calculated (Table 2). In this study, we interpret odds ratios (OR) and their 95% confidence intervals (CIs) as indicators of each feature's discriminative ability. The OR for "Platelet distribution width", "Procalcitonin", and features "CRP", "PaO2", and "Alkaline phosphatase" approximate 1, indicating weak associations with the outcome of interest. Notably, "CRP" and "PaO2" display statistically significant p-values in univariate analysis (p=0.019 and <0.01, respectively), suggesting predictive power despite modest OR. In multivariate analysis, "CRP" and "PaO2" remain significant (p= 0.006 and 0.013, respectively), with "CRP" showing slight attenuation in OR (from 1.003 to 0.994) and "PaO2" demonstrating a more substantial decrease (from 1.007 to 0.982). Features such as "Age", "Platelet distribution width", "Red blood cell distribution width", and "Triglyceride" exhibit OR significantly greater than 1 in both univariate and multivariate settings, indicating strong associations with the outcome. Notably, "Platelet distribution width" and "Red blood cell distribution width" have particularly high OR in multivariate analysis (1.353 and 1.266, respectively), underscoring their predictive utility. Conversely, "Gold grade" and "Smoke"

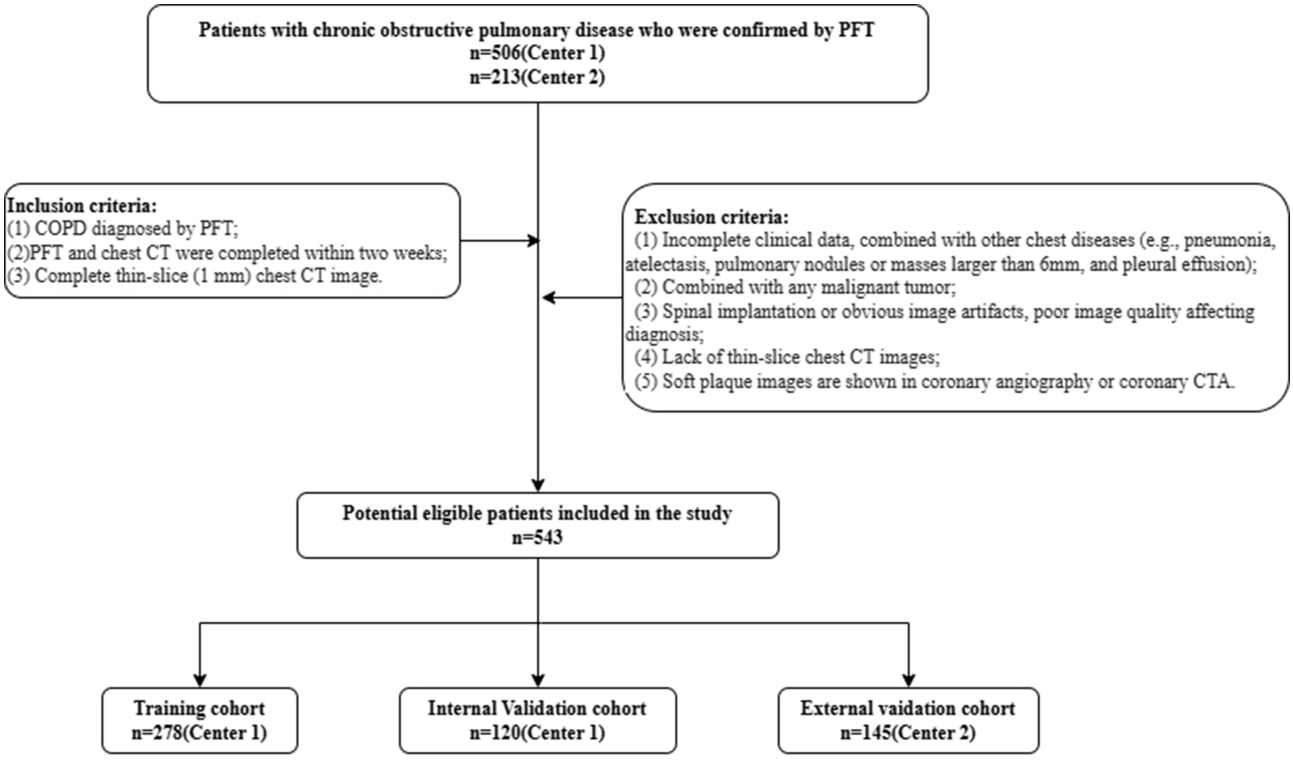

Figure 2 The flowchart of the patient's selection.

 https://doi.org/10.2147/COPD.S539307

https://doi.org/10.2147/COPD.S539307

Table 1 Baseline Characteristics of the Study Population

Clinical Factors		Training Cohort (n=278)			Internal Validation Cohort (n=120)			External Validation Cohort (n=145)		
		COPD without CHD(n=94)	COPD with CHD(n=184)	p-value	COPD without CHD(n=40)	COPD with CHD(n=80)	p-value	COPD without CHD(n=32)	COPD with CHD(n=113)	p-value
Age		73.90±8.48	75.54±6.50	0.216	73.72±9.31	76.45±6.49	0.065	73.66±8.42	75.26±6.60	0.258
Smoke		0.70±0.46	0.59±0.49	0.061	0.75±0.44	0.57±0.50	0.062	0.75±0.44	0.64±0.48	0.236
BMI		21.62±3.70	22.33±3.62	0.102	20.06±2.90	22.90±3.50	<0.001	21.97±7.26	22.54±7.17	0.815
C-Reactive Protein		98.48±73.38	73.68±70.39	0.008	101.65±73.34	76.65±78.56	0.048	108.91±77.99	155.48±84.15	0.008
Albumin		37.41±3.78	38.69±4.47	0.018	37.97±4.09	38.96±4.24	0.224	36.58±4.07	36.61±3.98	0.978
Globulin		26.48±4.32	27.59±4.82	0.061	27.00±4.54	28.01±4.20	0.229	25.72±4.39	26.48±4.21	0.375
Triglyceride		0.87±0.42	1.54±4.93	<0.001	0.82±0.46	1.20±0.80	<0.001	6.77±32.98	1.82±7.04	0.237
Alkaline Phosphatase		78.16±25.34	80.47±23.57	0.499	79.10±23.93	76.69±24.00	0.891	79.02±37.61	68.81±19.73	0.359
White blood cell count		6.96±2.53	6.71±3.43	0.139	6.86±2.43	6.15±2.05	0.201	7.55±3.83	7.14±4.89	0.334
Neutrophilic granulocyte percentage		72.94±12.32	68.54±12.16	0.005	73.69±11.97	67.72±10.64	0.008	71.33±12.21	66.26±13.68	0.024
Percentage of lymphocytes		18.14±9.35	20.83±9.24	0.012	17.91±10.14	21.89±8.68	0.009	16.89±6.47	20.54±9.53	0.061
Absolute eosinophil count		12.45±15.03	15.12±14.61	0.009	9.70±9.70	14.51±14.35	0.076	13.53±11.54	16.73±15.80	0.557
Plateletcrit		2.08±18.34	0.18±0.05	0.148	0.19±0.07	0.18±0.05	0.905	0.20±0.08	0.18±0.06	0.401
Red blood cell distribution width		13.29±1.19	13.57±1.44	0.086	13.13±0.98	13.67±1.79	0.039	13.07±1.03	13.47±1.17	0.057
Mean platelet volume		10.11±1.45	10.11±1.37	0.891	10.17±1.32	10.51±1.43	0.221	10.79±1.28	10.81±1.25	0.666
Platelet Distribution Width		15.85±1.35	16.12±0.89	0.065	15.95±1.59	15.97±1.68	0.631	13.03±2.97	13.66±2.46	0.121
Erythrocyte Sedimentation Rate		11.93±12.54	9.13±7.33	0.361	11.43±12.42	9.45±11.95	0.708	14.97±21.81	9.71±9.06	0.488
Procalcitonin		7.95±12.47	3.48±6.30	0.165	8.05±13.15	3.02±5.43	0.098	5.59±8.12	4.07±6.24	0.221
Arterial Oxygen Partial Pressure		92.28±26.12	85.44±13.67	0.371	96.43±30.95	89.35±22.33	0.879	86.60±20.13	82.92±16.65	0.431
Arterial Carbon Dioxide Partial Pressure		42.21±7.23	40.69±3.44	0.179	44.15±9.85	40.70±2.20	0.153	43.31±5.17	40.71±4.31	0.023
GOLD grade				<0.001			<0.001			0.059
	GOLDI	8(8.51)	48(26.09)		4(10.00)	22(27.50)		4(12.50)	12(10.62)	
	GOLDII	33(35.11)	58(31.52)		6(15.00)	25(31.25)		7(21.88)	18(15.93)	
	GOLDIII	32(34.04)	60(32.61)		17(42.50)	29(36.25)		10(31.25)	64(56.64)	
	GOLDIV	21(22.34)	18(9.78)		13(32.50)	4(5.00)		11(34.38)	19(16.81)	
Gender				0.031			0.691			0.065
	Female	9(9.57)	38(20.65)		7(17.50)	18(22.50)		0	15(13.27)	
	Male	85(90.43)	146(79.35)		33(82.50)	62(77.50)		32(100.00)	98(86.73)	

Table 2 Univariable and Multivariable Analysis of Clinical Features

Variable	Univariable analysis		Multivariable analysis	
	OR[95% CI]	p-value	OR[95% CI]	p-value
Procalcitonin	0.993[0.974,1.012]	0.541		
C-Reactive Protein	1.003[1.001,1.004]	0.019	0.994[0.99,0.997]	0.006
Arterial Oxygen Partial Pressure	1.007[1.004,1.009]	<0.01	0.982[0.969,0.994]	0.013
Alkaline Phosphatase	1.008[1.006,1.011]	<0.01	1.001[0.99,1.012]	0.883
Age	1.009[1.006,1.012]	<0.01	1.052[1.017,1.088]	0.013
Neutrophilic granulocyte percentage	1.009[1.006,1.011]	<0.01	0.926[0.875,0.979]	0.025
Arterial Carbon Dioxide Partial Pressure	1.015[1.01,1.02]	<0.01	0.952[0.903,1.003]	0.117
Albumin	1.018[1.013,1.024]	<0.01	1.011[0.945,1.081]	0.796
Erythrocyte Sedimentation Rate	1.023[1.007,1.039]	0.019	0.961[0.934,0.988]	0.017
Globulin	1.026[1.018,1.034]	<0.01	1.024[0.965,1.088]	0.516
BMI	1.032[1.022,1.042]	<0.01	1.044[0.973,1.12]	0.312
Absolute eosinophil count	1.032[1.02,1.044]	<0.01	0.986[0.965,1.007]	0.28
Percentage of lymphocytes	1.035[1.024,1.046]	<0.01	0.93[0.87,0.994]	0.073
Platelet Distribution Width	1.044[1.03,1.058]	<0.01	1.353[1.078,1.699]	0.029
Red blood cell distribution width	1.052[1.036,1.068]	<0.01	1.266[1.061,1.511]	0.028
Mean platelet volume	1.067[1.046,1.09]	<0.01	0.922[0.765,1.111]	0.472
White blood cell count	1.084[1.053,1.116]	<0.01	1.043[0.96,1.132]	0.405
GOLD	1.194[1.104,1.293]	<0.01	0.675[0.506,0.901]	0.025
Smoke	1.636[1.265,2.115]	0.002	0.874[0.477,1.605]	0.716
Gender	1.718[1.373,2.149]	<0.01	0.481[0.203,1.142]	0.164
Triglyceride	2.007[1.642,2.455]	<0.01	2.042[1.224,3.404]	0.022

exhibit contrasting patterns: "Gold grade" has a high OR in univariate analysis (1.194) but a lower and significant OR in multivariate analysis (0.675), while "Smoke" has a high OR in univariate analysis (1.636) but a non-significant OR in multivariate analysis (0.874). The contrasting patterns for "Gold grade" and "Smoke" between univariate and multivariate analyses suggest confounding variables may influence their associations. Overall, our results provide valuable insights into feature predictive utility and can inform future research and clinical decision-making.

Feature Selection and Model Construction

Based on CT images, radiomics features and 3D deep learning features were extracted, respectively. According to the ICC test results, 850 radiomics features and 2048 DL features were retained, respectively. After the *t*-test, Spearman correlation and LASSO, the radiomics features were finally screened out as the 10 best radiomics features (Figure 3A–C), and the radiomics model was constructed, using the following formula to filter radiomics features (Supplementary Material 3).

To improve the prediction accuracy of the risk of CHD in patients with COPD, we integrated radiomics features and deep learning features. After t-tests, Spearman correlation and LASSO regression, 9 features with non-zero coefficients were screened out (Figure 3D–F). And a deep learning model of radiomics was constructed, We use the following formula to filter DLR features (Supplementary Material 4). Finally, we combined this model with the clinical features we selected and developed a combined model using Logistic regression (LR). Figure 4 is a nomogram specifically designed for clinical use, where the total score corresponds to the probability of concurrent CHD risk in patients with COPD.

Comparison of Clinical Models, Radiomics Models, DLR Models and Nomogram Models

The performances of the clinical model, radiomics model, deep learning-radiomics model and nomogram model are shown in Table 3. For the training cohort, the Combined signature exhibits the highest AUC at 0.848, followed closely by DLR at 0.831 and Rad at 0.826. The clinic, with an AUC of 0.771, performs relatively lower. In the internal validation

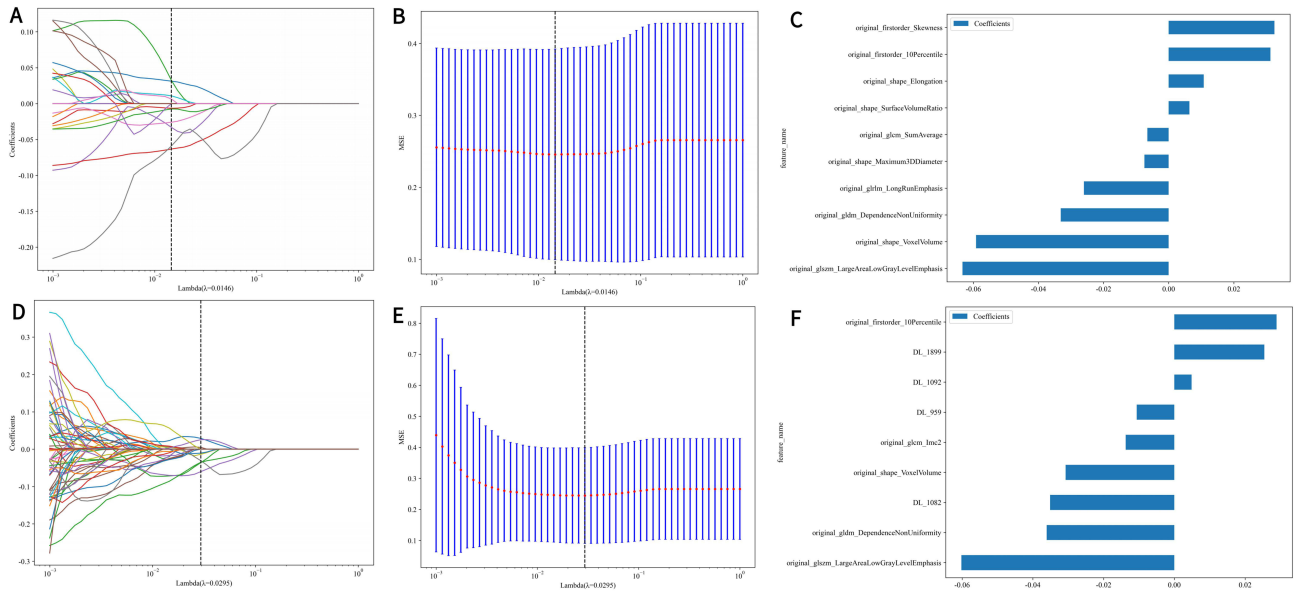

Figure 3 (**A** and **D**) represent the LASSO for radiomics and DLR features. (**B** and **E**) represent the MSE for radionics and DLR features. (**C** and **F**) represent the feature weights for radionics and DLR features.

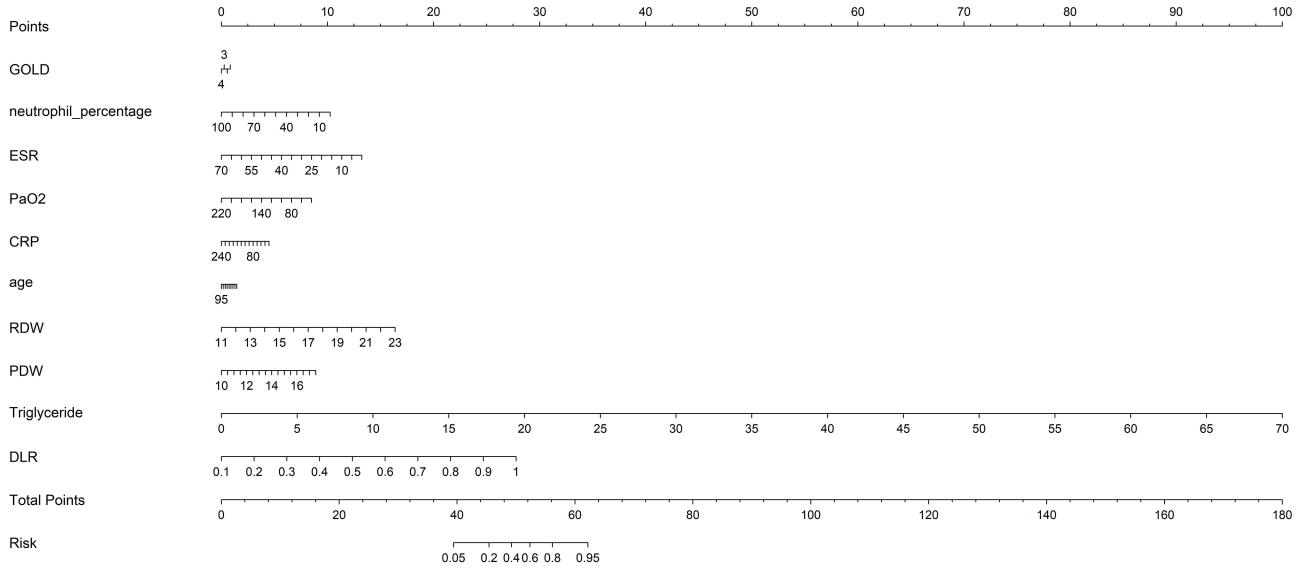

Figure 4 Clinical application of nomogram in the risk prediction of concurrent CHD.

cohort, the Combined signature again achieves the highest AUC at 0.8, with DLR and Rad closely trailing at 0.767 and 0.752, respectively. The clinic has an AUC of 0.759. For the external validation cohort, the highest AUC is observed for the Combined signature at 0.761, followed by DLR at 0.732. Rad and Clinic perform similarly with AUCs of 0.666 and 0.661, respectively. These results suggest that the Combined signature generally performs best across different cohorts in terms of AUC, indicative of its robustness and generalizability. Figure 5 shows the ROC curve of different models. Figure 6 shows Decision Curve Analysis (DCA), The overall net benefit of the combined nomogram on different queues in identifying the risk of coronary heart disease in COPD patients is higher than that of the clinical factor model, and this model covers most of the reasonable threshold probability range. Figure 7 shows the calibration curves, which demonstrate the consistency between the predicted and observed CHD in the two cohorts. Figure 8 shows the DeLong test. The results indicate that the nomogram model exhibits excellent predictive performance.

Table 3 The Performance of Four Models in the Different Cohorts. The Clinic, Clinical Model Signature; Rad, Radiomics Signature; DLR, Deep Learning Radiomics Signature; Combined, Combined Clinical, Deep Learning and Radiomics Signatures

	Accuracy	AUC	95% CI	Sensitivity	Specificity	PPV	NPV	Precision	Recall	F1	Threshold	Cohort
Clinic	0.745	0.771	0.7099–0.8311	0.783	0.67	0.823	0.612	0.823	0.783	0.802	0.624	Train
Rad	0.763	0.826	0.7754–0.8759	0.761	0.766	0.864	0.621	0.864	0.761	0.809	0.643	Train
DLR	0.791	0.831	0.7795–0.8824	0.842	0.691	0.842	0.691	0.842	0.842	0.842	0.663	Train
Combined	0.827	0.848	0.7964–0.8989	0.886	0.713	0.858	0.761	0.858	0.886	0.872	0.564	Train
Clinic	0.783	0.759	0.6597–0.8578	0.825	0.7	0.846	0.667	0.846	0.825	0.835	0.629	val
Rad	0.633	0.752	0.6622–0.8413	0.5	0.9	0.909	0.474	0.909	0.5	0.645	0.741	val
DLR	0.717	0.767	0.6769–0.8572	0.65	0.85	0.897	0.548	0.897	0.65	0.754	0.721	val
Combined	0.758	0.8	0.7108–0.8892	0.7	0.875	0.918	0.593	0.918	0.7	0.794	0.738	val
Clinic	0.715	0.661	0.5297–0.7932	0.757	0.538	0.875	0.341	0.875	0.757	0.812	0.437	Test
Rad	0.73	0.666	0.5379–0.7940	0.775	0.538	0.878	0.359	0.878	0.775	0.823	0.605	Test
DLR	0.657	0.732	0.6235–0.8411	0.613	0.846	0.944	0.338	0.944	0.613	0.743	0.701	Test
Combined	0.635	0.761	0.6562–0.8656	0.586	0.846	0.942	0.324	0.942	0.586	0.722	0.624	Test

Discussion

This study developed a nomogram model utilizing DLR features alongside clinical characteristics to identify high-risk individuals susceptible to coronary heart disease (CHD) among patients with chronic obstructive pulmonary disease (COPD). The nomogram demonstrated impressive area under the curve (AUC) values of 0.848, 0.8, and 0.761 in the training cohort, internal validation cohort, and external validation cohort, respectively. In comparison to single models, the nomogram exhibited superior calibration and discrimination capabilities. Its application may facilitate early identification of CHD risk and enable timely intervention and management strategies, thereby enhancing the overall net benefit

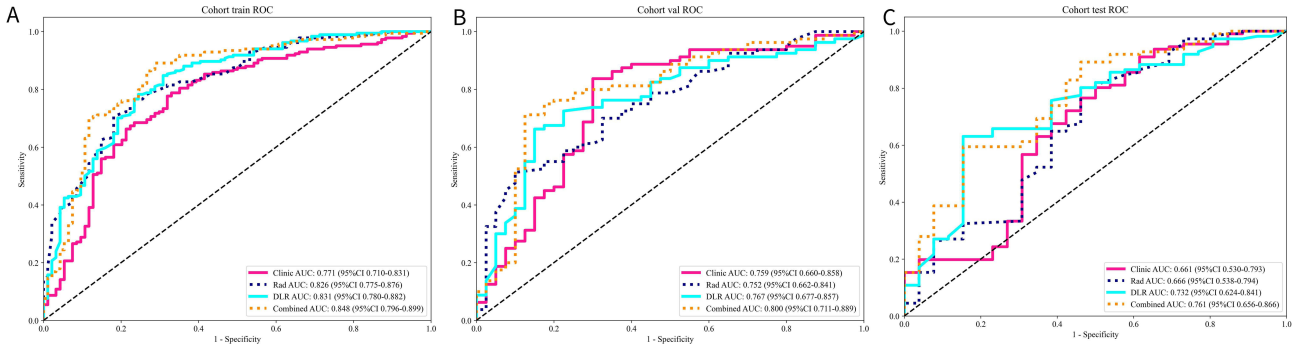

Figure 5 ROC curve of different models in the (**A**) train, (**B**) internal validation, and (**C**) external validation cohort, respectively.

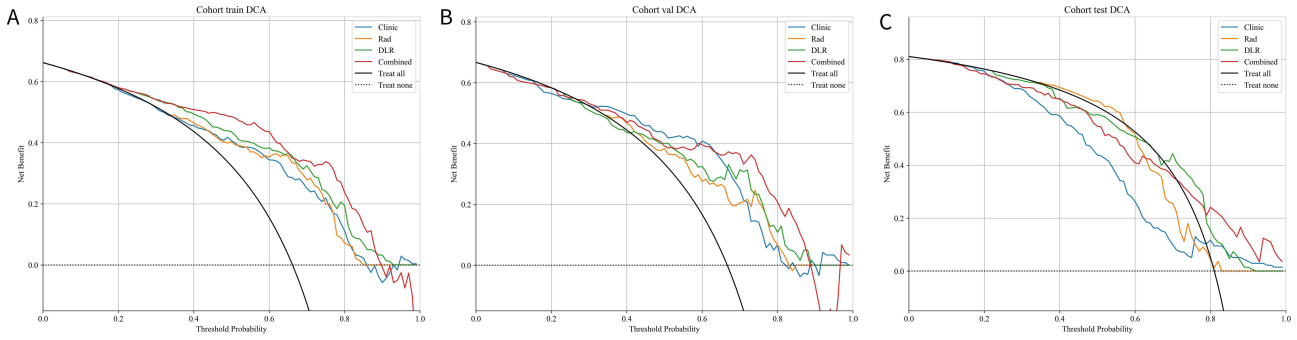

Figure 6 DCA curve of different models in the (**A**) train, (**B**) internal validation, and (**C**) external validation cohort, respectively.

https://doi.org/10.2147/COPD.S539307

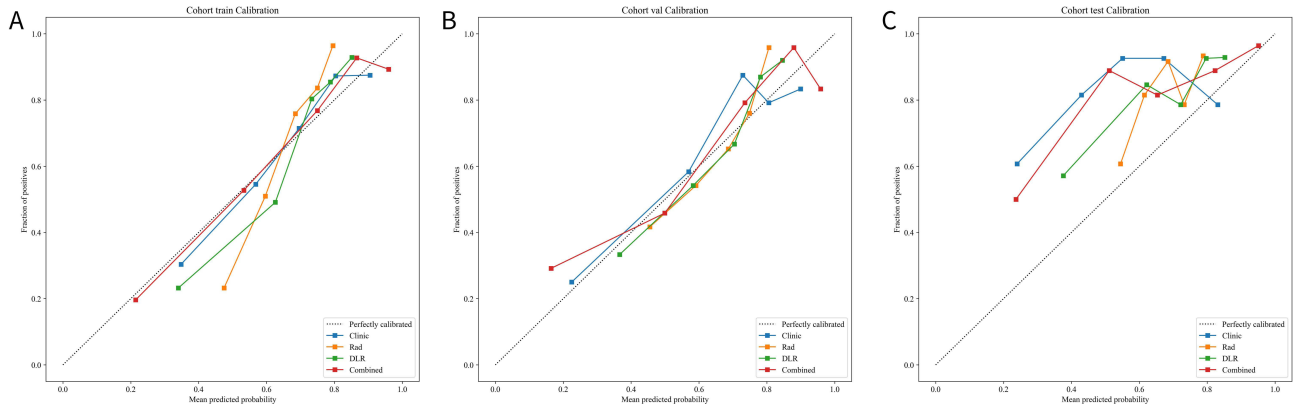

Figure 7 Calibration curve of different models in the (**A**) train, (**B**) internal validation, and (**C**) external validation cohort, respectively.

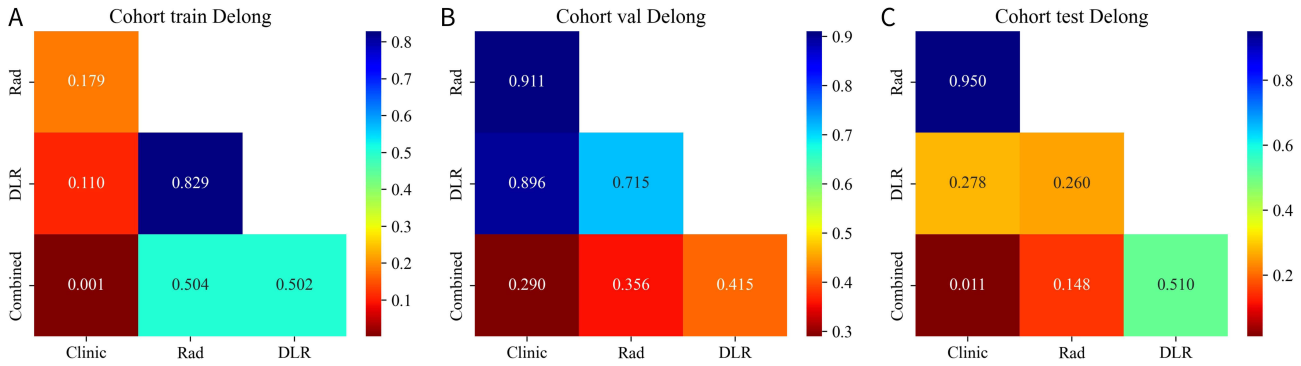

Figure 8 Delong test of different models in the (**A**) train, (**B**) internal validation, and (**C**) external validation cohort, respectively.

for COPD patients. COPD and CHD share anatomical proximity within the heart and lungs; numerous studies have established that COPD is a significant risk factor for CHD. Reactive oxygen species released by inflammatory cells oxidize lipids adhered to blood vessel walls, thus promoting atherosclerosis progression.[20] The coexistence of these two conditions further exacerbates patient prognosis.[21] Currently, approximately 59% of patients with severe COPD remain undiagnosed for CHD,[22] as many clinicians may overlook symptoms such as dyspnea or chest discomfort—attributing them instead to COPD-related manifestations[23]—which consequently increases both incidence rates and mortality associated with CHD.[24] Therefore, it is crucial to assess whether COPD patients also present with CHD. Research indicates that COPD patients participating in pulmonary rehabilitation programs experience a reduced risk of developing CHD,[25] underscoring the importance of early detection regarding potential risks in this population—particularly during acute exacerbations of COPD. This study employs a retrospective analysis approach; through early screening via chest CT scans, we identified COPD patients at high risk for CHD—thereby reducing screening costs while improving timeliness in disease management.

In recent years, numerous studies have concentrated on the association between chronic obstructive pulmonary disease (COPD) and coronary heart disease (CHD) mechanisms.[26] The prediction of the risk of concurrent COPD and CHD is primarily derived from clinical data. Several investigations have indicated that gender serves as an independent predictor of cardiovascular disease (CVD) in patients with COPD.[27,28] However, in our study, gender was not included in the model construction due to its non-significant p-value ($p = 0.164$), which may be attributed to the relatively low proportion of women within the cohort (16.0%). Research has established that smoking is a prevalent influencing factor for both COPD and CHD,[7] with higher smoking rates observed among men compared to women; consequently, COPD is also more frequently diagnosed in males.[29] In this study, smoking was excluded as an independent variable from the clinical model. We performed univariate and multivariate logistic regression analyses on clinical features to identify

independent predictors and subsequently developed a predictive model utilizing machine learning techniques. Our clinical model achieved an area under the curve (AUC) of 0.771, comparable to previously constructed models based solely on clinical data. To enhance the efficacy of our predictive framework, we sought alternative methods for extracting relevant predictors. Therefore, we integrated clinical features with radiomic characteristics and deep learning attributes to establish a combined model that outperformed individual models.

To our knowledge, there are limited studies utilizing chest CT for radiomics to identify coronary heart disease (CHD) in patients with chronic obstructive pulmonary disease (COPD). Lin et al[30] developed a combined model that integrates clinical features and radiomic characteristics, achieving an area under the curve (AUC) of 0.731 to predict the cardiovascular disease risk in COPD patients. Our study advances this research by specifically investigating the association between COPD and CHD while incorporating deep learning features into the combined model, resulting in an AUC of 0.848. In comparison to the clinical model (AUC = 0.731), radiomics model (AUC = 0.828), and deep learning radiomics (DLR) model (AUC = 0.831), our combined model demonstrates superior efficacy. The performance of the combined model was robust across training, internal validation, and external validation cohorts, as evidenced by high AUC values and favorable calibration curves; thus, it can be provisionally assumed that it possesses certain predictive capabilities. This multicenter study includes an independent external validation cohort to ensure its generalizability. Future research will focus on evaluating both the predictive performance and clinical utility of this model through prospective studies. Additionally, we plan to monitor real-time performance during application to ensure consistency between new data outcomes and those observed during training phases before optimizing the model accordingly.At present, there is a relatively mature Atherosclerotic Cardiovascular Disease (ASCVD) Risk Score in clinical practice. However, the advantage of our model lies in integrating COPD-specific indicators (such as BNP, pulmonary function classification, and blood gas analysis). From the perspective of efficacy, our model has a better predictive effect for patients with moderate to severe COPD.

We must recognize the limitations of our study. Firstly, due to the retrospective nature of this study, there may be potential confounding factors and biases. At the same time, some laboratory indicators were partially missing, and we used the average value to fill in. Secondly, due to the imbalance of each classification, COPD lung function indicators for which COPD risk classification could be improved were not classified. Future research should have a larger sample size and be balanced in classification. Thirdly, this study only studied lung features to determine the CHD risk of COPD patients and did not evaluate the effectiveness of mediastinal features. Future research should include models based on mediastinal features and compare them with models based on lungs.

Conclusion

This study employed automatic segmentation of whole lung parenchyma from computed tomography (CT) examinations conducted on COPD patients and proposed a nomogram that amalgamates clinical characteristics alongside radiomics and deep learning features. The objective is to predict the risk of concurrent CHD in individuals suffering from COPD—an endeavor anticipated to furnish clinicians with more accurate and practical tools for assessing CHD risk while adding supplementary value to chest CT images obtained from these patients. Furthermore, this investigation corroborated the relationship between CHD and COPD. Future research will aim at expanding sample sizes, integrating quantitative features, and employing advanced deep-learning methodologies for further optimization of our predictive model.

Ethical Approval

This retrospective study using anonymized medical record data received an Institutional Review Board (IRB) waiver of informed consent from the First People's Hospital of Huzhou, as it involves no direct patient intervention and adheres to the Declaration of Helsinki. Patient privacy is fully protected, and ethical standards are strictly maintained.

Funding

This work was supported by the Science and Technology Project of Huzhou City, Zhejiang Province (2023GY33) and Postgraduate Research and Innovation Project of Huzhou University (2025KYCX99).

Disclosure

The authors report no conflicts of interest in this work.

References

1. Halpin DMG. Mortality of patients with COPD. *Expert Rev Respir Med*. 2024;18(6):381–395. doi:10.1080/17476348.2024.2375416
2. Xu J, Ji Z, Zhang P, et al. Disease burden of COPD in the Chinese population: a systematic review. *Ther Adv Respir Dis*. 2023;17:17534666231218899. doi:10.1177/17534666231218899
3. Kahnert K, Jörres RA, Behr J, Welte T. The diagnosis and treatment of COPD and its comorbidities. *Dtsch Arztebl Int*. 2023;120(25):434–444. doi:10.3238/arztebl.m2023.027
4. Vespasiani-Gentilucci U, Pedone C, Muley-Vilamu M, et al. The pharmacological treatment of chronic comorbidities in COPD: mind the gap! *Pulm Pharmacol Ther*. 2018;51:48–58. doi:10.1016/j.pupt.2018.06.004
5. Ställberg B, Janson C, Larsson K, et al. Real-world retrospective cohort study Arctic shows the burden of comorbidities in Swedish COPD versus non-COPD patients. *NPJ Prim Care Respir Med*. 2018;28(1):33. doi:10.1038/s41533-018-0101-y
6. Brassington K, Selemidis S, Bozinovski S, Vlahos R. New frontiers in the treatment of comorbid cardiovascular disease in chronic obstructive pulmonary disease. *Clin Sci*. 2019;133(7):885–904. doi:10.1042/CS20180316
7. Chen H, Luo X, Du Y, et al. Association between chronic obstructive pulmonary disease and cardiovascular disease in adults aged 40 years and above: data from NHANES 2013–2018. *BMC Pulm Med*. 2023;23(1):318. doi:10.1186/s12890-023-02606-1
8. Vogelmeier CF, Friedrich FW, Timpel P, et al. Impact of COPD on mortality: an 8-year observational retrospective healthcare claims database cohort study. *Respir Med*. 2024;222:107506. doi:10.1016/j.rmed.2023.107506
9. Zhou TH, Zhou XX, Ni J, et al. CT whole lung radiomic nomogram: a potential biomarker for lung function evaluation and identification of COPD. *Mil Med Res*. 2024;11(1):14. doi:10.1186/s40779-024-00516-9
10. Lambin P, Leijenaar RTH, Deist TM, et al. Radiomics: the bridge between medical imaging and personalized medicine. *Nat Rev Clin Oncol*. 2017;14(12):749–762. doi:10.1038/nrclinonc.2017.141
11. Mayerhoefer ME, Materka A, Langs G, et al. Introduction to Radiomics. *J Nucl Med*. 2020;61(4):488–495. doi:10.2967/jnumed.118.222893
12. Amudala Puchakayala PR, Sthanam VL, Nakhmani A, et al. Radiomics for improved detection of chronic obstructive pulmonary disease in low-dose and standard-dose chest CT scans. *Radiology*. 2023;307(5):e222998. doi:10.1148/radiol.222998
13. Makimoto K, Hogg JC, Bourbeau J; CanCOLD Collaborative Research Group, et al. Enhancing COPD classification using combined quantitative computed tomography and texture-based radiomics: a CanCOLD cohort study. *ERJ Open Res*. 2024;10(4):00968–2023. doi:10.1183/23120541.00968-2023
14. Lukhumaidze L, Hogg JC, Bourbeau J, et al. Quantitative CT imaging features associated with stable PRISm using machine learning. *Acad Radiol*. 2025;32(1):543–555. doi:10.1016/j.acra.2024.08.030
15. Lin X, Zhou T, Ni J, et al. CT-based radiomics nomogram of lung and mediastinal features to identify cardiovascular disease in chronic obstructive pulmonary disease: a multicenter study. *BMC Pulm Med*. 2025;25(1):121. doi:10.1186/s12890-025-03568-2
16. Zhu Z, Zhao S, Li J, et al. Development and application of a deep learning-based comprehensive early diagnostic model for chronic obstructive pulmonary disease. *Respir Res*. 2024;25(1):167. doi:10.1186/s12931-024-02793-3
17. Christenson SA, Smith BM, Bafadhel M, Putcha N. Chronic obstructive pulmonary disease. *Lancet*. 2022;399(10342):2227–2242. doi:10.1016/S0140-6736(22)00470-6
18. Halpin DMG, Criner GJ, Papi A, et al. Global initiative for the diagnosis, management, and prevention of chronic obstructive lung disease. The 2020 GOLD science committee report on COVID-19 and chronic obstructive pulmonary disease. *Am J Respir Crit Care Med*. 2021;203(1):24–36. doi:10.1164/rccm.202009-3533SO
19. Brown KH, Ghita-Pettigrew M, Kerr BN, et al. Characterisation of quantitative imaging biomarkers for inflammatory and fibrotic radiation-induced lung injuries using preclinical radiomics. *Radiother Oncol*. 2024;192:110106. doi:10.1016/j.radonc.2024.110106
20. Expert Group of the Chronic Obstructive Pulmonary Disease Assembly; Chinese Thoracic Society, Chinese Medical Association. Chinese expert consensus on the management of cardiovascular comorbidities in patients with chronic obstructive pulmonary disease, *Zhonghua Jie He He Hu Xi Za Zhi*. 2022;45(12):1180–1191. Chinese. PMID: 36480848. doi:10.3760/cma.j.cn112147-20220505-00380
21. Yu G, Liu L, Ma Q, et al. Bidirectional causal association between chronic obstructive pulmonary disease and cardiovascular diseases: a Mendelian randomization study. *Int J Chron Obstruct Pulmon Dis*. 2024;19:2109–2122. PMID: 39351082; PMCID: PMC11439898. doi:10.2147/COPD.S475481
22. Reed RM, Eberlein M, Girgis RE, et al. Coronary artery disease is under-diagnosed and under-treated in advanced lung disease. *Am J Med*. 2012;125(12):1228.e13–1228.e22. PMID: 22959785; PMCID: PMC3732035. doi:10.1016/j.amjmed.2012.05.018
23. Svendsen CD, Kuiper KKJ, Ostridge K, et al. Factors associated with coronary heart disease in COPD patients and controls. *PLoS One*. 2022;17(4):e0265682. PMID: 35476713; PMCID: PMC9045629. doi:10.1371/journal.pone.0265682
24. Hawkins NM, Peterson S, Ezzat AM, et al. Control of cardiovascular risk factors in patients with chronic obstructive pulmonary disease. *Ann Am Thorac Soc*. 2022;19(7):1102–1111. PMID: 35007497. doi:10.1513/AnnalsATS.202104-463OC
25. Chen JO, Liu JF, Liu YQ, et al. Effectiveness of a perioperative pulmonary rehabilitation program following coronary artery bypass graft surgery in patients with and without COPD. *Int J Chron Obstruct Pulmon Dis*. 2018;13:1591–1597. PMID: 29805258; PMCID: PMC5960241. doi:10.2147/COPD.S157967
26. Bian H, Zhu S, Xing W, et al. Research status and direction of chronic obstructive pulmonary disease complicated with coronary heart disease: a bibliometric analysis from 2005 to 2024. *Int J Chron Obstruct Pulmon Dis*. 2025;20:23–41. doi:10.2147/COPD.S495326
27. Qiu Y, Wang Y, Shen N, et al. Nomograms for predicting coexisting cardiovascular disease and prognosis in chronic obstructive pulmonary disease: a study based on NHANES data. *Can Respir J*. 2022;2022:5618376. PMID: 35721788; PMCID: PMC9203208. doi:10.1155/2022/5618376
28. Lee SJ, Yoon SS, Lee MH, et al. Health-screening-based chronic obstructive pulmonary disease and its effect on cardiovascular disease risk. *J Clin Med*. 2022;11(11):3181. PMID: 35683565; PMCID: PMC9181412. doi:10.3390/jcm11113181

29. Zhao X, Kang H, An Y, et al. Whole-course management of chronic obstructive pulmonary disease in primary healthcare: an internet of things-enabled prospective cohort study in China. *BMJ Open Respir Res*. 2024;11(1):e001954. doi:10.1136/bmjresp-2023-001954
30. Lin X, Zhou T, Ni J, et al. CT-based whole lung radiomics nomogram: a tool for identifying the risk of cardiovascular disease in patients with chronic obstructive pulmonary disease. *Eur Radiol*. 2024;34(8):4852–4863. doi:10.1007/s00330-023-10502-9